stein modes with $\vec{k} \perp \vec{B}$ in inhomogenous plasma columns under conditions similar to the present experiment are described by K. Mitani, H. Kubo, and S. Tanaka, J. Phys. Soc. Japan 19, 211 (1964); S. J. Buchsbaum and A. Hasegawa, Phys. Rev. Letters 12, 685 (1964), and Phys. Rev. 143, 303 (1966); F. W. Crawford, G. S. Kino, and H. H. Weiss, Phys. Rev. Letters 13, 229 (1964); S. Gruber and G. Bekefi, Phys. Fluids 11, 122 (1968).

[5]The plasma was the positive column of an 0.8-cm-i.d. hot-cathode discharge in Ar or Hg at pressures below 10 mTorr. The pump and stimulated radiation propagated in a waveguide in the TE_{01} mode. Magnetic field homogeneity was better than 0.2% over the section of the discharge contained by the waveguide.

[6]Coupling between extraordinary and plasma waves near the upper hybrid frequency was observed by A. Y. Wong and A. F. Kuckes, Phys. Rev. Letters 13, 306 (1964), and discussed by T. H. Stix, ibid. 15, 878 (1965), and H. H. Kuehl, Phys. Rev. 154, 124 (1967). Absorption and stimulated emission at the upper hybrid frequency was directly measured by R. M. Hill, D. E. Kaplan, and S. K. Ichiki, Phys. Rev. Letters 19, 154 (1967). The latter also report the unexplained observation that excitation at ω_{uh} yielded stimulated emission at frequencies $\leq \omega_{uh}$.

[7]S. Gruber, Phys. Fluids 11, 858 (1968); the appearance of modes with $\omega \geq 2\omega_c$ due to a particle-wave instability excited by radiation at $\omega_0 \sim \omega_c$ is described by Anastassiades and Marshall, Ref. 2.

[8]S. M. Hamberger, A. Malein, J. H. Adlam, and M. Friedman, Phys. Rev. Letters 19, 350 (1967).

DIFFUSION IN TOROIDAL PLASMAS WITH RADIAL ELECTRIC FIELD

T. E. Stringer
United Kingdom Atomic Energy Authority, Culham Laboratory, Berkshire, England
(Received 16 January 1969)

The equilibrium of an axisymmetric toroidal plasma is analyzed. In the resistive regime the diffusion rate derived by Pfirsch and Schlüter is modified when the plasma rotates about its minor axis because of electric drift. In the weakly collisional regime the electron-diffusion rate is greater than that derived by Galeev and Sagdeev, except in the ambipolar condition where the diffusion rate is comparable with theirs.

The drift motions of ions and electrons in a toroidal magnetic field lead to a charge separation in a toroidal plasma which must be neutralized by current flow along the magnetic field. When finite resistivity is included this neutralization is not complete. Pfirsch and Schlüter[1] have shown that the residual electrostatic field can lead to a large enhancement of the diffusion rate compared with that in a comparable straight plasma column. In this and other papers[2,3] on resistive diffusion in tori any density variation over magnetic surfaces due to finite ion inertia is neglected. The weak collisional case, where collisions are too infrequent to produce an effective resistivity but are enough to prevent toroidally trapped particle orbits, was investigated recently by Galeev and Sagdeev.[4] Here Landau damping replaces resistivity. These authors include the density perturbation, but neglect any potential variation, over magnetic surfaces. This note considers the equilibrium of resistive and weakly collisional toroidal plasmas, including both density and potential variation over magnetic surfaces. Radial electrostatic fields producing rotation of the toroidal plasma around its minor axis, which are observed in most toroidal confinement experiments, are included in the equilibrium.

The coordinate system, illustrated in Fig. 1, and magnetic field are the same as discussed in Ref. 2. Relative to the (r, θ, φ) coordinates the magnetic field is taken to be

$$\vec{B} = (R_0/R)[0, B_{0\theta}(r), B_{0\varphi}], \tag{1}$$

where R_0 is the radius of the magnetic axis, $R = R_0(1+\epsilon\cos\theta)$, and $\epsilon = r/R_0$. The displacement of magnetic surfaces relative to the magnetic axis in a realistic toroidal field will be neglected for simplicity. Since the aspect ratio will be assumed large, the equilibrium density and potential may be expanded as a series in ϵ:

$$n(r,\theta) = n_0(r) + n_1(r,\theta) + \cdots,$$

$$\Phi(r,\theta) = \Phi_0(r) + \Phi_1(r,\theta) + \cdots. \tag{2}$$

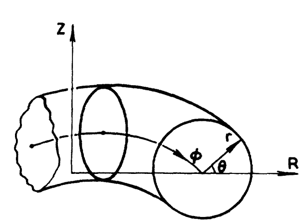

FIG. 1. The coordinates.

Axial symmetry is assumed. It can be confirmed from the later equations that the zero-order density and potential must be constant over magnetic surfaces. Their radial distribution will be regarded as known, and the θ-dependent corrections which result inevitably from the toroidal-field variation will be deduced. Temperature is assumed constant.

Resistive plasma equilibrium.—Guiding-center equations will be used. The effect of finite-Larmor-radius corrections on the equilibrium is generally small and will be neglected in the following analysis. The mean guiding-center velocity of each species may be written in the form

$$\vec{v}_j = v_{j\parallel}\vec{B}/|B| + \vec{v}_{bj} + \vec{v}_0 + \vec{v}_1 + \cdots, \tag{3}$$

where

$$\vec{v}_{bj} = -\frac{2\kappa T_j}{e_j BR}\vec{e}_z,$$

$$\vec{v}_0 = -\frac{\nabla\Phi_0 \times \vec{B}}{B^2}, \quad \vec{v}_1 = \frac{\nabla\Phi_1 \times \vec{B}}{B^2}, \cdots.$$

The usual guiding-center collisional diffusion across the field due to unlike particle collisions, which contributes a diffusion equal to that in a straight plasma column,[1] is omitted for brevity. $\vec{e}_z$ is a unit vector in the z direction.

We now substitute Eq. (3) in the guiding-center continuity equations $\nabla\cdot(n\vec{v}_j) = 0$, retaining only first-order terms in ϵ (the zero-order terms vanish). Both $\vec{v}_b$ and $\vec{v}_0$ contribute first-order terms as follows:

$$\nabla\cdot(n\vec{v}_{bj}) = -\frac{2\kappa T_j}{e_j BR}\frac{dn_0}{dr}\sin\theta,$$

$$\nabla\cdot(\vec{v}_0) = -\nabla\left(\frac{1}{B^2}\right)\cdot(\nabla\Phi_0 \times \vec{B}) + \frac{(\nabla\times\vec{B})\cdot\nabla\Phi_0}{B^2}$$

$$= -\frac{2}{R}v_{0\theta}\sin\theta. \tag{4}$$

Since $\nabla\times\vec{B}$ is in the φ direction, $(\nabla\times\vec{B})\cdot\nabla\Phi_0 = 0$. Thus

$$(\vec{v}_0\cdot\nabla)n_1 + (\vec{v}_1\cdot\nabla)n_0 + n_0\frac{\partial v_{j\parallel}}{\partial s} = \frac{2}{R}\left(\frac{p_j'}{e_j B} + n_0 v_{0\theta}\right)\sin\theta, \tag{5}$$

where

$$\frac{\partial}{\partial s} = \frac{1}{B}(\vec{B}\cdot\nabla) = \frac{B_\theta}{rB}\frac{\partial}{\partial\theta} = \frac{\epsilon\iota}{2\pi}\frac{1}{r}\frac{\partial}{\partial\theta}. \tag{6}$$

Since the mean guiding-center motion parallel to the magnetic field is identical to the fluid velocity, the fluid equation of motion and the generalized Ohm's law may be used to describe this motion:

$$\frac{nm_i}{r}v_{0\theta}\frac{\partial v_{i\parallel}}{\partial\theta} = -\kappa(T_i + T_e)\left(\frac{\epsilon\iota}{2\pi}\right)\frac{1}{r}\frac{\partial n_1}{\partial\theta}, \tag{7}$$

$$\eta j_\parallel = \left(\frac{\epsilon\iota}{2\pi}\right)\frac{\partial}{\partial\theta}\left[-\Phi_1 + \frac{\kappa T_e}{n_0 e}n_1\right]. \tag{8}$$

Subtracting Eq. (5) for the ions and electrons gives

$$j_\parallel = -\frac{2\pi}{\iota}\frac{2p'}{B_0}\cos\theta. \tag{9}$$

After substituting for $j_\parallel$ in Eq. (8), n_1 and Φ_1 may readily be obtained from Eqs. (7), (8), and the ion continuity Eq. (5). For example,

$$n_1 = \frac{2\epsilon n_0}{Dv_{0\theta}}\left[-(U_{in} + v_{0\theta})\cos\theta + \frac{\eta n_0' p' r}{n_0 B^2}\left(\frac{2\pi}{\epsilon\iota}\right)^2\sin\theta\right], \tag{10}$$

where

$$D = 1 + \frac{U_{en}}{v_{0\theta}} - \frac{c_s^2}{v_{0\theta}^2}\left(\frac{\epsilon\iota}{2\pi}\right)^2,$$

$$U_{jn} = \frac{\kappa T_j}{e_j B}\frac{n_0'}{n_0}, \quad c_s^2 = \frac{\kappa(T_i + T_e)}{m_i}. \tag{11}$$

The average outward flux across a magnetic surface is

$$nv_{Dj} = \frac{1}{2\pi r B_0}\int_0^{2\pi}(n_0 + n_1)\left(\frac{\partial\Phi_1}{\partial\theta} + \frac{2\epsilon\kappa T_j}{e_j}\sin\theta\right) \times (1 + \epsilon\cos\theta)^2 d\theta \tag{12}$$

$$= \frac{2n_0\eta p'}{B_0^2 D}\left(\frac{2\pi}{\iota}\right)^2\left[\frac{c_s^2}{v_{0\theta}^2}\left(\frac{\epsilon\iota}{2\pi}\right)^2 + \frac{U_{in} - U_{jn}}{v_{0\theta}}\right]. \tag{13}$$

The factor D in the denominator of Eqs. (10) and (13) may be understood as follows. In the plasma frame the toroidal field structure appears as an $m = 1$ field variation rotating with angular velocity $-v_{0\theta}/r$. Its wavelength along the field lines corresponds to a wave number $k_\parallel = \epsilon\iota/2\pi r$. The density accumulation produced by this field variation will drive a forced oscillation of the plasma, traveling in phase with the field variation. The response of the plasma is inversely proportional to its dielectric constant. If the dielectric constant in the rest frame of the plasma is $D(\omega, k_\parallel)$, then its response to the toroidal field variation will be inversely proportional to $D(-v_0\theta/r, \epsilon\iota/2\pi r)$. The factor D is the dielectric constant for ion-acoustic drift waves in an inhomogeneous plasma.

When $v_0 \to 0$ the diffusion rate agrees with that derived by Pfirsch and Schlüter.[1] When $D \to 0$, corresponding to the condition where the wavelength and Doppler-shifted frequency seen by the plasma coincide with a natural mode, the diffusion will be much faster than the Pfirsch-Schlüter rate. When finite-Larmor-radius effects and ion-ion collisions are included in the analysis, the factor D acquires a dissipative component which would limit the response to resonant excitation. However, these effects are very weak in experimental conditions of interest. In practice the resonant response will be limited by non-linear effects, or by ion Landau damping which is discussed in the next section.

The Pfirsch-Schlüter diffusion rate clearly satisfies energy balance, in that the resulting decrease in plasma internal energy just balances the Ohmic dissipation ηj^2.[1,3] When density varies over magnetic surfaces the Ohmic dissipation $E_\parallel j_\parallel$ may be greater than $\eta j_\parallel{}^2$ because of the pressure gradient in Eq. (8). In addition, the zero-order electric drift transfers energy to the plasma equal to $\int dr \int \vec{v}_0 \cdot \nabla p dS$, whose sign is that of D. Thus when $D<0$ the plasma feeds energy into the electrostatic field, while when $D>0$ it extracts it. This partly explains the apparent anomaly that when $D>0$ the diffusion given by Eq. (13) is inwards. A potential distribution making $D>0$ would have to feed energy continually into the plasma to maintain the E/B rotation. Such a potential could therefore not occur naturally.

Weak collisional-plasma equilibrium. – If the mean free path exceeds the connection length $2\pi r/\epsilon\iota$, collisional resistivity becomes ineffective. The kinetic equations must then be used to include any resonant particle effects. The equilibrium and diffusion are significantly different depending on whether collisions are sufficient to prevent particle trapping in the toroidal field.[4] Only the case $\epsilon^{-3/2} > \lambda_{\rm mfp}\epsilon\iota/2\pi r > 1$, where no trapped particles exist, will be considered here. Collisions do not enter the analysis explicitly, but are necessary to justify the assumption of a Maxwellian velocity distribution for particles near the resonant velocity $v_\parallel = -v_0 2\pi/\epsilon\iota$. The analysis follows similar lines to the resistive problem, but is appreciably more complex. The details will be published separately. Only an outline can be given here, but the similarity of the results to those derived for the simpler resistive problem may make them more plausible.

Taking a distribution function of the form $f = f_0 \times (r, \vec{v}) + f_1(r, \theta, \vec{v})$, where $f_1 = O(\epsilon f_0)$, the kinetic equation is solved for f_1 in terms of Φ_1. Integrating f_1 gives the azimuthally varying part of the density $n_1(r,\theta)$ as defined in Eq. (2). Invoking quasineutrality $(n_{i1} = n_{e1})$ gives an equation for $\Phi_1(r,\theta)$, the θ-dependent part of the potential. Φ_1 is given by the real part of the equation

$$\Phi_1 = \frac{\epsilon\kappa T_e}{ev_0(F+iL)}[U_{in}I(z_i) - U_{en}I(z_e) - U_{in}(1+\tau) + v_0\{I(z_i) - I(z_e)\} + 2(U_{in}+v_0)z_i^2 I(z_i)]e^{i\theta}, \tag{14}$$

where

$$I(z) = 1 - 2ze^{-z^2}\int_0^z e^{t^2}dt + i\sqrt{\pi}ze^{-z^2},$$

$$z_j = -\frac{v_0}{c_j}\frac{2\pi}{\epsilon\iota}, \quad c_j = \left(\frac{2\kappa T_j}{m_j}\right)^{1/2}, \quad \tau = \frac{T_e}{T_i}, \quad F + iL = [(U_{en}+v_0)I(z_e) + \tau(U_{in}+v_0)I(z_i)]/v_0.$$

$F+iL$ may be recognized as the dielectric constant for an $m=1$ drift ion-acoustic mode with frequency $-v_0/r$ and parallel wave number $\epsilon\iota/2\pi r$ in a collisionless plasma. The imaginary term in $I(z_i)$ results from the singularity in $f_{1j}(v_\parallel)$ at $v_\parallel = -v_0 2\pi/\epsilon\iota$. When f_1 is integrated over $v_\parallel$ this singularity gives rise to a Landau-type term. Such particles have zero azimuthal velocity and so are "resonant" with the stationary field structure.

The radial diffusion is obtained from an equation similar to Eq. (12), except that now because of its velocity dependence the curvature drift must be integrated over $f_1(\theta, v_\parallel)$. The average radial fluxes of ions and electrons across magnetic surfaces are found to be

$$nv_{Di} = -\frac{\sqrt{\pi}\,\epsilon a_i^2 c_i}{8}\frac{2\pi}{r}\frac{}{\iota}\left(1+\frac{v_0}{U_{in}}\right)\exp(-z_i^2)\left[1+\frac{S(S+\tau)}{F^2+L^2}\right]\frac{dn_0}{dr}, \tag{15}$$

$$nv_{De} = -\frac{\sqrt{\pi}\,\epsilon a_i^2 c_i \tau}{8}\frac{2\pi}{r}\frac{}{\iota}\left[\left(1+\frac{v_0}{U_{in}}\right)\frac{S\exp(-z_i^2)}{(F^2+L^2)} + \left(1+\frac{v_0}{U_{en}}\right)\left(\tau\frac{m_e}{m_i}\right)^{1/2}\left\{1+\frac{G^2+L^2(1+\tau+2z_i^2)^2/\tau^2}{F^2+L^2}\right\}\right]\frac{dn_0}{dr}, \tag{16}$$

where

$$S = 1+\tau+2z_i^2(1+U_{en}/v_0), \quad G = (1+\tau)\left[I_{0i}-(1-I_{0i})\frac{U_{in}}{v_0}\right]+2z_i^2\left(1+\frac{U_{in}}{v_0}\right)I_{0i},$$

and

$$I_{0i} = 1-2z_i\exp(-z_i^2)\int_0^{z_i} e^{t^2}\,dt$$

is the real part of $I(z_i)$.

The ion diffusion rate is proportional to the ion Landau term, while the electron diffusion contains terms proportional to both the ion and electron Landau terms [the latter have a factor $(m_e/m_i)^{1/2}$]. This differs from the result obtained by Galeev and Sagdeev[4] for this regime. Their ion diffusion rate is of the same order as given by Eq. (15), but their electron diffusion rate contains only electron Landau terms and so tends to be less than the ion rate because of the factor $(m_e/m_i)^{1/2}$. This difference results from the neglect of a θ-dependent potential $\Phi_1(\theta)$ in their analysis. The ions and electrons are then decoupled and the diffusion rate for each species is determined by the Landau damping for that species. Since their electron and ion densities do not vary equally over magnetic surfaces, hence not conserving quasineutrality, the neglect of Φ_1 is inconsistent. The radial drift resulting from $\partial\Phi_1/\partial\theta$ in Eq. (12) is common to both species and gives a common diffusion component proportional to the ion Landau term.

Although the ion and electron diffusion rates are generally comparable, it may be seen from Eqs. (15) and (16) that when the electron Landau term is neglected, the ion rate always exceeds the electron rate. If there is no other source of loss, a radial space-charge field will quickly build up to bring the two rates to equality. Equating Eqs. (15) and (16) gives the following equations for the ambipolar potential distribution and the ambipolar diffusion rate (assuming $z_i \lesssim 2$):

$$\frac{v_0}{U_{in}} = -1+\frac{(1+\tau)}{(1+2z_i^2+2z_i^4)}\left(\tau\frac{m_e}{m_i}\right)^{1/2}\exp(-z_i^2), \tag{17}$$

$$nv_{Da} = -\frac{\sqrt{\pi}\,\epsilon a_i^2 c_i}{8}\frac{2\pi}{r}\frac{}{\iota}\left(\tau\frac{m_e}{m_i}\right)^{1/2}\left[2(1+\tau)+\frac{\tau(1+2z_i^2)}{1+2z_i^2+2z_i^4}\right]\frac{dn_0}{dr}. \tag{18}$$

Although for general v_0 the diffusion rate of both species tends to be dominated by the ion Landau term, the ambipolar potential reduces the coefficient $(1+v_0/U_{in})\exp(-z_i^2)$, which is common to all ion Landau terms, to a value of order $(m_e/m_i)^{1/2}$. The resulting ambipolar rate is thus proportional to the electron Landau term and is comparable with that given by Galeev and Sagdeev.

Comparison with experiments. – The preceding analysis may be extended to stellarators by superimposing a helical field on the toroidal variation. The expansion procedure used is equivalent to a linearization in ϵ_t and ϵ_h, and so the diffusion produced by each field variation is independent of the other. With existing stellarator parameters the toroidal diffusion is dominant.

With the exception of Wendelstein II, the measured diffusion in all existing stellarators exceeds the earlier theoretical estimates by one or two orders of magnitude. In those with $l = 3$ windings the connection length is generally such that the resistive theory should apply over most of the cross section. The resonant enhancement over the Pfirsch-Schlüter rate requires a central potential several times $\kappa T/e$, which is consistent with observation. At larger radii, where the weak-collisional theory should in some cases be applicable, lack of closure of the magnetic surfaces may allow an enhanced electron diffusion rate to balance the higher ion diffusion rate. The preceding theory thus provides a plausible explanation of the observed diffusion in these devices.

[1]D. Pfirsch and A. Schlüter, Max-Planck Institute Report No. MPI/PA/7/62, 1962 (unpublished).
[2]G. Knorr, Phys. Fluids 8, 1334 (1965).
[3]M. D. Kruskal and R. M. Kulsrud, Phys. Fluids 1, 265 (1958).
[4]A. A. Galeev and R. Z. Sagdeev, Zh. Eksperim. i Theor. Fiz. 53, 348 (1967) [translation: Soviet Phys. – JETP 26, 233 (1968)].

CLUSTERING EFFECTS AND THE RIGID-BAND MODEL IN Cu-Ni ALLOYS

A. Kidron
Physics Department, Technion—Israel Institute of Technology, Haifa, Israel
(Received 7 October 1968)

Cu-Ni alloys contain clusters of one type of atom. These clusters have a mean size of 44 atoms in an almost equiatomic alloy, annealed for 50 h at 300°C. At least 18% of the alloy undergoes this segregation. These results are in accordance with many physical properties of these alloys but throw some doubt on the conclusions of recent works about the inapplicability of the rigid-band model to this system.

There have been many studies[1-3] of the physical properties of Cu-Ni alloys showing indirectly that these solid solutions must include Ni-rich clusters with a magnetic moment even in the range of composition where the solid solution is not ferromagnetic. Recently there have also been several studies[4-6] on the optical properties of Cu-Ni alloys with the explicit purpose of checking the applicability of the rigid-band model[7] to this system. We show here that these solid solutions include clustered zones of one type of atom and that one cannot rely too much on the discussion of the results of the optical measurements. We feel that the disagreement of the results with the rigid-band model is still not conclusive.

In a recent work[8] using small-angle scattering of x rays we have shown that there is clustering of the atoms in Cu-Ni alloys. Fourier analysis of the relative intensity gives $p_{AA}(r)$, the probability of finding an atom of type A at a distance r from a given A atom. The plot of $p_{AA}(r)$ as a function of r is similar to the one seen in Al-Ag and in Al-Zn in the very first stage of precipitation.[9]

There is another approach to the interpretation of this scattering.[10] We assume spherical particles with a radius R_1 and a concentration C_1 of one type of atom, say A, these particles being surrounded by a spherical shell of outer radius R_2 and a concentration C_2 of A atoms. In this model the intensity of the small-angle scattering per cm^3 of the sample is given by

$$I=Nn^2(f_A-f_B)^2 \times[\exp(S^2R_1{}^2/10)-\exp(S^2R_2{}^2/10)]^2, \quad (1)$$

where N is the number of particles per cm^3. n is given by

$$n=(\tfrac{4}{3}\pi R_1{}^3)\frac{4}{a^3}(C_1-C_2)=(\tfrac{4}{3}\pi R_2{}^3)\frac{4}{a^3}(C_0-C_2), \quad (2)$$

where a is the lattice parameter, C_0 is the mean concentration of A atoms, $S=4\pi\sin\theta/\lambda$, with θ the Bragg angle and λ the wavelength of the radiation, and f_A, f_B are the scattering factors of the A and B atoms, respectively.

We see that starting from zero Bragg angle the intensity will rise with increasing angle, go through a maximum at some angle θ_m, and then decrease at higher angles. This behavior of the intensity is seen in Fig. 1, where we plot the logarithm of the intensity as a function of S^2. The plot is for the intensity per atom and is given in electron units, i.e., in units of the Thomson scattering of one electron. For values of θ higher than θ_m the intensity can be approximated by

$$I=Nn^2(f_A-f_B)^2\exp[-S^2R^2/5]. \quad (3)$$

This approximation should not be good for relatively very high values of $\sin\theta/\lambda$, where the scattering falls down with S^{-4}.

In Fig. 1 we see than $\ln I$ is linear after θ_m. From the slope of the line we find $R_1=4.9$ Å and from its intercept at $S^2=0$ we get $Nn^2=2.8\times10^{22}$ cm^{-3}. Differentiating (1) with respect to S we find a relation between R_1, R_2, and $S_m=4\pi\sin\theta_m/\lambda$. Taking θ_m from the intensity plot and the value of R_1 we find $R_2=30$ Å. Putting the values of R_1 and R_2 in (2) we get a relation between C_1 and C_2 ($C_0=0.50$). In our alloy C_1 is somewhere be-